Liquid Crystals
Publication details, including instructions for authors and subscription information:
http://www.tandfonline.com/loi/tlct20

New heteropolynuclear metallomesogens: copper(II), palladium(II), nickel(II) and oxovanadium(IV) chelates with [3]ferrocenophane-containing Schiff's base and β-aminovinylketone

Hye Won Chae [a], Oleg N. Kadkin [a] & Moon-Gun Choi [a]
[a] Department of Chemistry and Centre for Bioactive Molecular Hybrids, BK21, Yonsei University, 134 Shinchon-Dong, Seodaemoon-Gu, Seoul 120-749, Korea
Published online: 19 Feb 2009.

To cite this article: Hye Won Chae, Oleg N. Kadkin & Moon-Gun Choi (2009) New heteropolynuclear metallomesogens: copper(II), palladium(II), nickel(II) and oxovanadium(IV) chelates with [3]ferrocenophane-containing Schiff's base and β-aminovinylketone, Liquid Crystals, 36:1, 53-60, DOI: 10.1080/02678290802650261

To link to this article: http://dx.doi.org/10.1080/02678290802650261

Liquid Crystals,
Vol. 36, No. 1, January 2009, 53–60

Taylor & Francis
Taylor & Francis Group

New heteropolynuclear metallomesogens: copper(II), palladium(II), nickel(II) and oxovanadium(IV) chelates with [3]ferrocenophane-containing Schiff's base and β-aminovinylketone

Hye Won Chae, Oleg N. Kadkin* and Moon-Gun Choi*

Department of Chemistry and Centre for Bioactive Molecular Hybrids, BK21, Yonsei University, 134 Shinchon-Dong, Seodaemoon-Gu, Seoul 120-749, Korea

(Received 20 September 2008; final form 26 November 2008)

New mesogenic heteropolynuclear complexes of Cu(II), Pd(II), Ni(II) and VO(IV) with the [3]ferrocenophane-containing Schiff's base, and Cu(II) and Pd(II) complexes with the [3]ferrocenophane-containing β-aminovinylketone have been synthesised. The obtained heterometallic mesogenes are identified by elemental analysis, proton nuclear magnetic resonance, infrared and ultraviolet–visible spectroscopies. Liquid crystalline properties are studied by thermal polarising optical microscopy and differential scanning calorimetry techniques. Both ligands and heteropolynuclear complexes exhibit thermotropic nematic and smectic C mesophases in various temperature ranges except for the Ni(II) complex. Mesomorphism of the prepared complexes is correlated with the geometry of their central chelate core. Considerably broader mesophases and lower transition temperatures are achieved in the synthesised metallomesogens by using the alkylidene-bridged ferrocene as a building unit.

Keywords: ferrocenophane; liquid crystal; metallomesogen; azomethine, aminovinylketone; Schiff's base; heteronuclear complex

1. Introduction

Metallomesogens are modern advanced materials with much potential attributed to the special properties of metal atoms (*1–6*). Various new molecular architectures can be realised in metal-containing liquid crystals that are difficult to achieve in conventional organic materials, such as square, folded square, lantern, pyramidal, octahedral geometrical shapes etc. Moreover, intermolecular coordinative interactions between transition metals in a similar manner to hydrogen bonds open an effective way to construct supramolecular assemblies. For instance, hydrogen bonding was efficiently applied to obtain ferrocene-containing supramolecular liquid crystals (*7, 8*). In general, a ferrocene unit has proven to be a valuable unit for the molecular design and synthesis of metallomesogen structures owing to its rich chemistry and three-dimensional architecture, and this was utilised in the numerous examples of ferrocene-containing liquid crystals (*9–17*). In our earlier works, we have synthesised and investigated heteropolynuclear metallomesogens using ferrocene derivatives as ligands for building up coordination complexes with transition metals (*18–21*). This approach uses the advantages of a ferrocene unit, such as chemical and thermal stability, three-dimensional structure and aromatic chemistry, to introduce additional metal centres into conventional metallochelates. Heteropolynuclear metallomesogens containing a wide range of different transition metals are of special interest, since such systems have been shown by Kahn to be prominent for generating ferromagnetism in molecular compounds (*22–24*). Interesting examples of intramolecular ferromagnetic coupling interactions have been found earlier in calamitic binuclear iron(III) complexes (*25*), and in binuclear copper(II) smectic (*26*) and discotic materials (*27*). Spin-coupling interactions were also observed in homobinuclear discotic metallomesogens involving both copper(II) and nickel(II) ions (*28, 29*). Studies on liquid crystalline systems with multiple metal centres are also essential to establish the fundamental relationships between their chemical structure, geometrical shapes and functional properties. This stimulated many researchers to design liquid crystalline heteropolynuclear (*30–35*) complexes with various molecular architectures.

The main purpose of the present work is the synthesis of new heteropolynuclear metallomesogens on the base of organometallic ligands with finely tuned molecular architecture. In the present study, a soft alkylidene bridge is introduced into the terminal ferrocene fragment, in contrast to earlier synthesised heteropolynuclear complexes with ferrocene-containing ligands, in order to improve thermal characteristics of the mesophases. It is well established that the

*Corresponding authors. Email: onk@yonsei.ac.kr; choim@yonsei.ac.kr

ISSN 0267-8292 print/ISSN 1366-5855 online

DOI: 10.1080/02678290802650261
http://www.informaworld.com

incorporation of a 1,3-propanediyl bridge between cyclopentadienyl rings in the ferrocenomesogenes allows broader mesophases and lower transition temperatures to be achieved (*36–38*). Copper(II), palladium(II), nickel(II) and oxovanadium(IV) metallochelates with two kinds of [3]ferrocenophane-containing ligands are reported herein. Most of the incorporated metal centres are paramagnetic. Therefore, the obtained heteropolynuclear metallomesogens are of considerable interest with regard to their magnetic properties and new effects in liquid crystalline materials.

2. Experimental details

All synthetic procedures were carried out using standard Schlenk techniques. Solvents were dried and freshly distilled just before use. Reagent grade chemicals and solvents were purchased from Aldrich, TCI and Fluka. Proton nuclear magnetic resonance (^{1}H-NMR) spectra were measured on a Bruker AM 400 with internal TMS standard. Fourier transform infrared (FT-IR) spectra were performed on Nicolet Abatar-360 FT-IR spectrometer. Differential scanning calorimetry (DSC) thermographs were obtained on Perkin Elmer Diamond DSC with a scan rate of 5°C a minute. Thermooptical observations were carried out on a Nicon Eclipse E600 Pol optical polarised microscope equipped with a Mettler Toledo FP82 HT hot stage system and Mettler FP90 central processor. Microphotographs were obtained with a Moticam 2300 digital camera. Ultraviolet (UV) and visible spectra in the region of 200–800 nm were recorded on a spectrophotometer Shimadzu UV-1650PC. Elemental analyses were performed on a Fisons instrument 2A1108 at Korea Institute of Science and Technology. Column chromatographic separations were carried out on neutral Al_2O_3 from Aldrich. Alumina TLC plates D-5160 Duran from Macherey-Nagel were used to selecting eluants and control the separation process. [3]Ferrocenophane **1** was obtained from [3]ferrocenopnan-2-one by reduction with $LiAlH_4$ (*39, 40*). [3]Ferrocenopnan-2-one was synthesised from ferrocene using a Turbitts–Watts one-step annelation procedure (*41*). Some modifications were added to the above-described procedures for the syntheses of 4-nitrophenyl[3]ferrocenophane (*42*) and 4-aminophenyl-[3]ferrocenophane (*37*). [3]Ferrocenophane-containing ligands **4** and **5** were synthesised according to the earlier described procedures (*37*).

2.1. Synthesis of 3-(4-nitrophenyl)[3]ferrocenophane (2)

4-Nitroaniline (3.04 g, 22 mmol) was dissolved under heating in 20 ml of 15% HCl (aq) and cooled to −5°C under vigorous stirring. Sodium nitrite (1.528 g, 22 mmol) in H_2O (5 ml) was added dropwise to a stirred suspension of the aniline, so the temperature in the reaction mixture was not allowed to rise higher than 0°C. The cold diazonium salt solution was added portion wise to a cold solution of ferrocenophane (5.00 g, 22 mmol) in 500 ml of diethyl ether containing hexadecyltrimethylammonium bromide (0.25 g, 0.68 mmol). The reaction mixture was stirred at 0°C for 6 h and then at room temperature overnight. The resulting mixture was transferred into a one-litre round-bottom flask and was treated with ascorbic acid to reduce ferricinium cations. Diethyl ether was evaporated thoroughly in a rotary evaporator. The obtained residue was extracted several times with ether and water. Then the ether layer was dried with Na_2SO_4 and filtered. Al_2O_3 (20g) was added to the obtained ethereal solution and the solvent was evaporated in a rotary evaporator. The adsorbed reaction products were placed on the top of Al_2O_3 column and eluted with hexane and toluene (10:3). The first fraction contained unreacted [3]ferrocenophane (1.88 g, 38%). The solvent from the second fraction was evaporated to dryness. The yield of the nitrocompound **2** after the column chromatography was 1.65 g (21%). It was recrystallised from ethanol. The purple crystals were filtered off and dried. The yield of the recrystallised material was 1.26 g (16%), the melting point was 123–124°C. ^{1}H-NMR (400 MHz, $CDCl_3$, 25°C): δ=2.00 (m, 6H, C_3H_6 bridge), 3.41 (m, 1H, C_5H_4Fe), 3.90 (m, 1H, C_5H_4Fe), 4.26 (m, 2H, C_5H_4Fe), 4.28 (m, 1H, C_5H_3Fe), 4.61 (m, 2H, C_5H_3Fe), 7.48 (d, J_1(H,H)=8 Hz, 2H, C_6H_4), 8.08 (d, J_1(H,H)=8 Hz, 2H, C_6H_4).

2.2. Synthesis of 3-(4-aminophenyl)[3]ferrocenophane (3)

We added Pd/C 10% (0.15 g) to a solution of 3-(p-nitrophenyl)[3]ferrocenophane **2** (1.26 g, 3.6 mmol) in a mixture of benzene/EtOH (2:1, 50 ml). The reaction mixture was shaken in a Paar-like hydrogenation apparatus under a hydrogen pressure of 3 atm for 6 h. A solution colour was changed from purple to yellow at the end of reaction. The resulting mixture was filtered through a celite layer, and then the solvents were evaporated. The obtained residue was purified by column chromatography on Al_2O_3 with diethyl ether/ethyl acetate (2:1). The yield was 0.86 g (74%) of yellowish orange powder; melting point 95°C. ^{1}H-NMR (200 MHz, $CDCl_3$, 25°C): δ=1.85−2.05 (m, 6H, C_3H_6 bridge), 3.41 (m, 1H, C_5H_3Fe), 3.20–3.70 (br. s, 2H, NH_2), 3.87 (m, 1H, C_5H_3Fe), 4.03 (m, 1H, C_5H_3Fe), 4.18 (m, 2H, C_5H_4Fe), 4.38 (m, 2H, C_5H_4Fe), 6.57 (m, 2H, C_6H_4), 7.22 (m, 2H, C_6H_4);

IR (KBr tablet): $\tilde{\nu} = 3458(N-H)$, 3368 (N–H), 2906.1 (C–H), 2835 (C–H), 1621, 1531, 1469, 1430, 1276, 1043, 829 cm^{-1}.

2.3. Synthesis of bis{4-[3]ferrocenophanophenyl-N-[4-(4-dodecyloxybenzoyloxy)salicylidene]iminato} copper(II) (6-Cu)

Schiff's base ligand **4** (0.050 g, 0.069 mmol) dissolved in hot n-butyl alcohol (2 ml) and $Cu(OAc)_2 \cdot H_2O$ (0.007 g, 0.035 mmol) dissolved in hot ethanol (2 ml) were mixed together in a 10 ml flask. The mixture was stirred and refluxed for 30 min. The yellowish brown precipitate of complex **6-Cu** was filtered off, washed with ethanol, and recrystallised from n-butyl alcohol. The yield was 0.041 g (78%). Elemental analysis for $C_{90}H_{100}CuFe_2N_2O_8$: calculated, C 71.44, H 6.66, N 1.85; found, C 71.30, H 6.64, N 2.09%.

2.4. Synthesis of bis{4-[3]ferrocenophanophenyl-N-[4-(4-dodecyloxybenzoyloxy)salicylidene]iminato} palladium(II) (6-Pd)

Schiff's base ligand **4** (0.050 g, 0.069 mmol) and $Pd(OAc)_2$ (0.008g, 0.035mmol) were dissolved in 1,4-dioxane (5 ml) with heating in an Ar atmosphere until dissolved and then stirred for 1 h at ambient temperature. Then ethanol was added to the reaction mixture, and a yellow precipitate was formed. The precipitate was filtered off, washed with ethanol, and recrystallised from n-butyl alcohol. The yield was 0.023 g (42%). ^{1}H-NMR (400 MHz, $CDCl_3$, 25°C) $\delta = 0.89$ (t, 3H, CH_3), 1.28 (m, 18H, CH_2) 1.81 (m, 2H, $C\underline{H_2}CH_2O$), 1.92 (m, 6H, C_3H_6, bridge), 3.44 (m, 1H, C_5H_4Fe), 3.77 (m, 1H, C_5H_4Fe), 4.02 (t, 2H, CH_2O), 4.07 (m, 1H, C_5H_3Fe), 4.11 (m, 2H, C_5H_4Fe), 4.53 (m, 2H, C_5H_3Fe), 6.07 (m, 1H, C_6H_3), 6.44 (dd, J_1(H,H) = 8 Hz, J_2(H,H) = 8 Hz, 1H, C_6H_3), 6.88 (d, J_1(H,H) = 8 Hz, 2H, C_6H_4) 7.22 (m, 4H, C_6H_4), 7.44 (d, J_1(H,H) = 8 Hz, 1H, C_6H_3), 7.73 (s, 1H, CH=N), 8.05 (d, J_1(H,H) = 8Hz, 2H, C_6H_4). Elemental analysis for $C_{90}H_{100}Fe_2N_2O_8Pd$: calculated, C 69.48, H 6.48, N 1.80; found, C 69.20, H 6.55, N 1.69%.

2.5. Synthesis of bis{4-[3]ferrocenophanophenyl-N-[4-(4-dodecyloxybenzoyloxy)salicylidene]iminato} nickel(II) (6-Ni)

Schiff's base ligand **4** (0.050 g, 0.069 mmol) in hot ethanol (2 ml) and excess $Ni(OAc)_2 \cdot 4H_2O$ (0.009 g, 0.036 mmol) in hot methanol (2 ml) were mixed together and refluxed for 2 h. The greenish yellow precipitate was filtered off, washed with ethanol, and recrystallised from n-butyl alcohol. The yield was 0.045 g (60%). Elemental analysis for $C_{90}H_{100}Fe_2N_2NiO_8$: calculated, C 71.67, H 6.68, N 1.86; found, C 71.57, H 6.66, N 2.17%.

2.6. Synthesis of bis{4-[3]ferrocenophanophenyl-N-[4-(4-dodecyloxybenzoyloxy)salicylidene]iminato} oxovanadium(IV) (6-VO)

$VOSO_4 \cdot 5H_2O$ (0.012 g, 0.048 mmol) in methanol (2 ml) and NaOAc (0.008 g, 0.096 mmol) in hot ethanol (2 ml) were mixed together, then a solution was filtered through a celite layer to a solution of Schiff's base ligand **4** (0.050 g, 0.069 mmol) in hot n-butyl alcohol (2 ml). The reaction mixture was refluxed for 1 h. Yellow precipitate was filtered off, washed with ethanol and recrystallised from n-butyl alcohol. The yield was 0.051 g (98%). Elemental analysis for $C_{90}H_{100}Fe_2N_2O_9V$: calculated, C 71.28, H 6.65, N 1.85; found, C 71.09, H 6.61, N 2.19%.

2.7. Synthesis of bis{4-[3]ferrocenophanophenyliminato-N-[1-(4-dodecyloxyphenyl)prop-1-enolate-3-ylidene]}copper(II) (7-Cu)

β-Aminovinylketone ligand **5** (0.050 g, 0.079 mmol) in hot n-butyl alcohol and $Cu(OAc)_2 \cdot H_2O$ (0.080 g, 0.040 mmol) in hot ethanol were mixed together, and stirred and refluxed for 30 min. The yellowish brown precipitate was filtered off, washed with ethanol, and recrystallised from n-butyl alcohol. The yield was 0.020 g (35%). Elemental analysis for $C_{80}H_{96}CuFe_2N_2O_4$: calculated, C 72.58, H 7.23, N 2.12; found, C 72.07, H 7.34, N 2.32%.

2.8. Synthesis of bis{4-[3]ferrocenophanophenyliminato-N-[1-(4-dodecyloxyphenyl)prop-1-enolate-3-ylidene]}palladium(II) (7-Pd)

β-Aminovinylketone ligand **5** (0.100 g, 0.158 mmol) and excess $Pd(OAc)_2$ (0.024 g, 0.12 mmol) were dissolved in hot 1,4-dioxane and stirred for 1 h. Ethanol was added to the resulting mixture and a yellow precipitate was formed. The precipitate was filtered off, washed with ethanol, and recrystallised from n-butyl alcohol. The yield was 0.09 g (90%). ^{1}H-NMR (400 MHz, $CDCl_3$, 25°C) $\delta = 0.89$ (t, 3H, CH_3), 1.28 (m, 18H, CH_2) 1.71 (m, 2H, $C\underline{H_2}CH_2O$), 2.03 (m, 6H, C_3H_6, bridge), 3.46 (m, 1H, C_5H_4Fe), 3.79 (t, 2H, CH_2O), 3.93 (m, 1H, C_5H_4Fe), 4.13 (m, 1H, C_5H_3Fe), 4.27 (m, 2H, C_5H_4Fe), 4.49 (m, 2H, C_5H_3Fe), 5.62 (d, J_1 (H,H) = 8 Hz, 1H, CO=CH), 6.56 (m, 2H, C_6H_4), 7.10 (d, J_1 (H,H) = 4 Hz, 1H, CH=N), 7.21 (m, 2H, C_6H_4) 7.39, (d, J_1 (H,H) = 8 Hz, 2H, C_6H_4). Elemental analysis for $C_{80}H_{96}Fe_2N_2O_4Pd$: calculated, C 70.30, H 7.01, N 2.05; found, C 70.05, H 7.26, N 2.47%.

3. Results and discussion

3.1. Synthesis and characterisation

The synthetic routes for the preparation of [3]ferrocenophane ligands and their transition metal complexes are outlined in Scheme 1. Arylation of [3]ferrocenophane **1** with appropriate diazonium salt in the presence of surfactant phase-transfer catalyst hexadecyltrimethylammonium bromide allowed us to obtain a reasonable yield of nitrocompound **2**. Subsequent reduction of **2** in a medium-pressure hydrogenation apparatus gave *p*-aminophenyl[3]ferrocenophane **3**, which can be further derivatised to mesogenic and promesogenic ligands **4** and **5** following the earlier described procedures (*37*). These chelating agents were reacted with different metal salts such as $Cu(OAc)_2$, $Pd(OAc)_2$, $Ni(OAc)_2$ and $VO(OAc)_2$ in suitable organic solvents. Thus, two series of heteropolynuclear systems **6** and **7** were generated. In the case of VO(IV) acetate the required salt was prepared from vanadyl(IV) sulfate immediately before use. Apparently, the preparation of corresponding complexes of Ni(II) and VO(IV) with the ligand **5** were unsuccessful by the procedures applied herein.

The obtained heteropolynuclear complexes were characterised by IR and UV–visible spectroscopies, and ^{1}H-NMR in the case of palladium(II) complexes. Elemental analyses of the complexes are consistent with the proposed structures. Significant high-field shifts of the signals of ligand protons which are close to the chelating core are observed in the complexes **6-Pd** and **7-Pd** compared with free ligands indicating the formation of coordination bonds on those sites.

Coordination of the metal ions to ligand **4** involves a salicylidene fragment and azomethine group. The corresponding changes can be outlined in relevant IR signals associated with the complexation of metals (see Table 1). Absorption bands of the valent stretching vibrations of the C=N bond are shifted in 13–14 cm^{-1} to the low-frequency region in all complexes in the series **6** compared with that of the

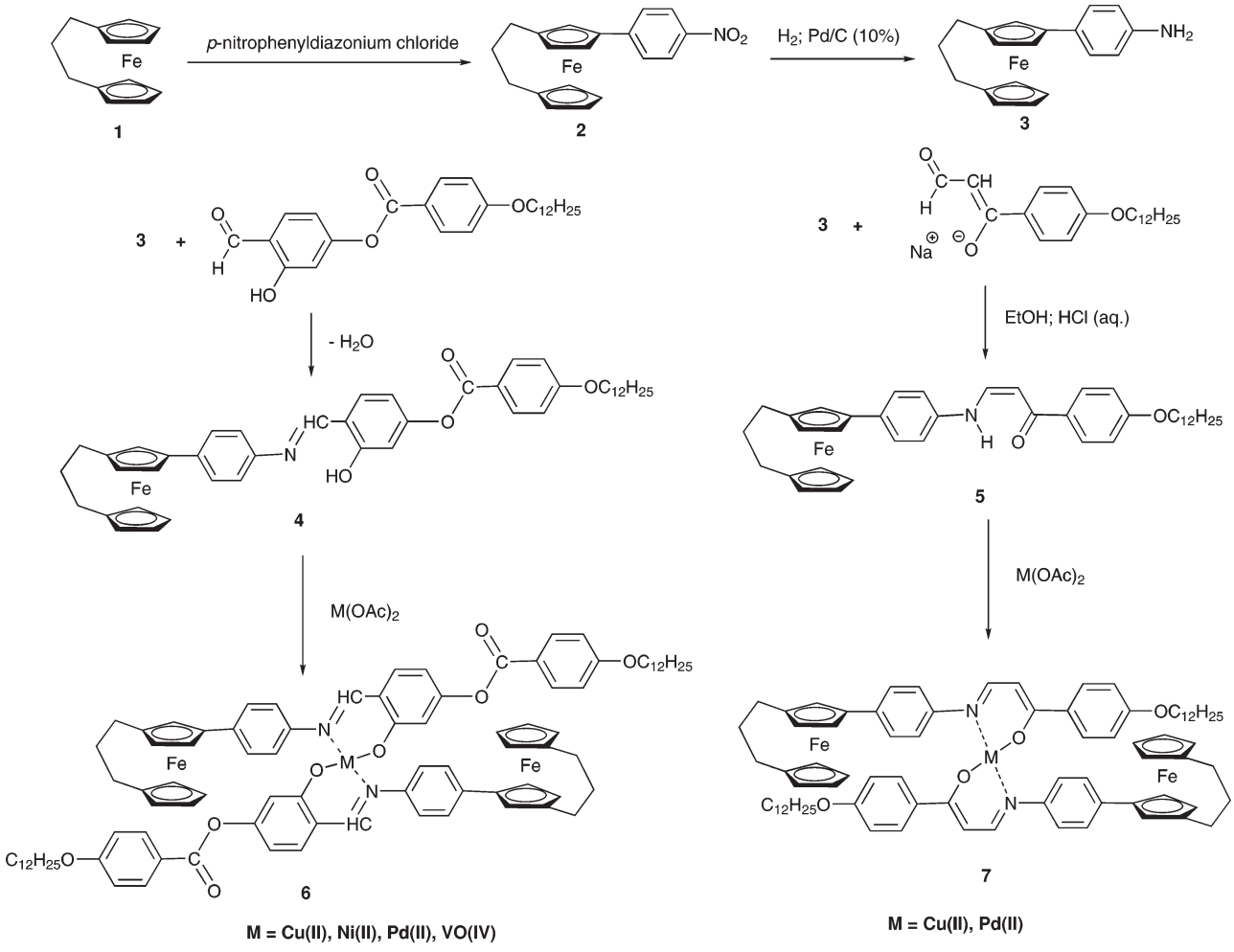

Scheme 1. Synthetic routes to [3]ferrocenophane-containing heteropolynuclear mesogenic complexes.

Table 1. Most relevant IR bands of ligand **4** and metal complexes **6**.

Compound	Vibration frequencies of functional groups (cm^{-1})				
	$\nu_{C=O}$	$\nu_{C=N}$	ν_{Ph-O}	δ_{O-M-N}, ν_{M-O}, ν_{M-N}	$\nu_{V=O}$
4	1725	1618	1320		
6-Cu	1732	1605	1310	611, 565, 476	
6-Pd	1735	1606	1304	617, 567, 469	
6-Ni	1735	1605	1311	591, 569, 468	
6-VO	1735	1605	1293	620, 567, 470	638

free ligand **4**. Analogous low-frequency shifts were observed for a stretching band of the Ph–O bonds varying from 9 cm^{-1} for **6-Ni** to 17 cm^{-1} for **6-VO**. Some weak absorption bands appear at around 470–620 cm^{-1}, which are attributed to stretching and bend deformations of newly formed M–O and M–N bonds. The vanadyl complex **6-VO** in addition show a stretching band corresponding to the V=O bond.

Three intensive absorption bands connected with valence vibrations of the C=O, C=N and C=C bonds can be seen clearly in the IR spectra of β-aminovinylketone **5** in the region around 1570–1630 cm^{-1} (see Table 2). The band of the C=O bond is not present in complexes **7**, that indicates coordination of the metal ions through the oxygen and nitrogen atoms and formation of metal-aromatic rings. The latter assumption is supported by emergence of whole series of very intensive absorption bands in the region around 1340–1565 cm^{-1} in complexes **7**. Those bands are absent in the free ligand **5**, and can be assigned in **7** to the deformations of the metal-aromatic cycles. It is worth noting that coordination of metal species in a case of **7** extends the rigidity of the central part of molecule by formation of the conjugated sequence of aromatic rings. An absorption band at 1574 cm^{-1} in **5**, associated with the stretching vibrations of the C=C bond, is shifted in complexes **7** by about 10 cm^{-1} to the higher-frequency region. Some weak bands related to the M–O and M–N bonds were observed upon complex formation in the region around 560–760 cm^{-1}.

UV–visible spectra of the Schiff's base ligand **4** and their transition metal complexes are represented by three groups of absorption bands (see Table 3): band I with a maximum near 350 nm is related to π–π* electronic transitions of the azomethine chromophor; band II in the region of 360–410 nm is associated with metal-to-ligand transitions of the [3]ferrocenophane unit and in the central chelate core; band III related to the absorption shoulders of lower intensity in the region of 450–470 nm, which is the result of d–d electronic transitions in the metal ions. The metal–ligand charge transfer bands in **6-Cu** and **6-Pd** have maxima at 410 nm, as for comparable salicylidene complexes with a square-planar geometry

Table 2. Most relevant IR bands of ligand **5** and metal complexes **7**.

Compound	Vibration frequencies of functional groups (cm^{-1})				
	$\nu_{C=O}$	$\nu_{C=N}$	$\nu_{C=C}$	$\delta_{M-Ar\ ring}$	ν_{M-O}, ν_{M-N}
5	1629	1600	1574		
7-Cu		1602	1586	1561, 1528, 1496, 1435, 1400, 1345	693, 586
7-Pd		1601	1585	1565, 1518, 1495, 1427, 1387, 1353	767, 565

Table 3. UV–visible (CH_2Cl_2) data of ligands **4** and **5** and metal complexes **6** and **7** (sh: shoulder).

Compound	λ_{max} (nm) (log ε, 1 cm^{-1} mol^{-1})		
	Band I	Band II	Band III
4	350 (4.595)	380 (sh) (3.679)	455 (sh) (3.949)
6-Cu	340 (sh) (4.456)	411(4.656)	479 (sh) (4.266)
6-Pd	342 (sh) (4.183)	410(4.237)	469 (sh) (3.893)
6-Ni	329 (sh) (4.738)	389 (4.668)	466 (sh) (4.054)
6-VO	319 (sh) (4.474)	362 (4.474)	459 (sh) (3.894)
5		392(4.760)	460 (sh) (4.062)
7-Cu		392(4.952)	440 (sh) (4.686)
7-Pd		395(4.723)	470 (sh) (4.066)

(*19*). The analogous band in complex **6-Ni** with a tetrahedral geometry has a maximum at 389 nm, and complex **6-VO** with a square-pyramidal geometry absorbs at 362 nm.

Both β-aminovinylketone ligand **5** and its complexes **7** showed strong absorption with maxima at around 390 nm belonging to π–π^* electronic transitions of the ligand chromophors, which are combined in a case of **7-Cu** and **7-Pd** with metal-to-ligand electronic transitions occurring apparently in the same region. The shoulders at 440–470 nm reveal d–d transitions in metal species.

Thus, new heteropolynuclear metallomesogens have been synthesised and characterised by elemental analyses and the spectroscopic methods. One kind of metal centre was incorporated into the free ligands by using alkylidene-bridged ferrocene, which is proven to be more efficient in comparison with unbridged ferrocene with regard to the liquid crystal properties (*36–38*). Then various transition metals were successfully coordinated to the chelating sites of the obtained organometallic compounds.

3.2. *Liquid crystal properties*

Liquid crystal properties of the synthesised new metallomesogens have been investigated by thermal polarising optical microscopy and DSC. The obtained data of thermal behaviour of ligands **4** and **5** and two series of neteronuclear complexes **6** and **7** are compiled in Table 4. Thermodynamic phase transitions and types of the mesophases were identified by characteristic optical textures observed in a thermal polarising microscope and enthalpy values in DSC thermograms. In general, the DSC thermogram peaks for a cooling process have lower enthalpy values than the corresponding item for a heating course. Following the same trend the crystallisation peaks did not appear in some cases. Apparently, that is connected with slower processes in the case of a transition to the more organised phases, and partial or complete vitrification of compounds upon cooling.

Most of the heteropolynuclear metal complexes of series **6** with the [3]ferrocenophane-containing Schiff's base **4**, except of the complex **6-Ni**, exhibited enantiotropic nematic mesophases with typical thread-like optical textures observed under a polarising microscope (see Figure 1). Phase transition temperatures are significantly higher in a case of complexes **6** in comparison with the free ligand **4**. This is not surprising considering significantly higher molecular weights upon complexation and the increased number of interacting sites. On the other hand, mesophase ranges became broader upon complexation, and this trend confirms that new molecular architectures brought by metallomesogen structures frequently enhance liquid crystal properties.

In addition, there are obvious variations of phase transition temperatures and mesomorphism depending on metal ions of the central chelate core (see Table 4). Several factors such as the size of the metal ions, the geometry of the complexes and the possibility of weak metal–metal intermolecular interactions may be responsible for these differences. The latter factor most likely causes exceptionally high phase transition temperatures for **6-Pd**. Regarding geometry, **6-Cu** and **6-Pd** have square-planar geometry which is favourable for liquid crystalline behaviour owing to the increased geometrical anisotropy of their molecules. At the same time **6-Ni** with unfavourable tetrahedral geometry and crossed alignment of the coordinated ligands does not show mesomorphism. Complex **6-VO** adopting a square-pyramidal configuration with the coordinated ligands positioned in one plane exhibited a nematic

Table 4. Phase transitions, temperatures (°C) and corresponding enthalpy changes (in parentheses, kJ mol^{-1}) of ligands **4** and **5** and complexes **6** and **7** (Cr: crystal; N: nematic phase; SmC: smectic C phase; I: isotropic liquid).

	Phase transitions	
Compound	Heating process	Cooling process
4[a]	Cr_1 137 (5.39 and −5.54) Cr_2 163 (41.05) N 177 (0.25) I	I 176 (−0.25) N 104 (−38.80) Cr
6-Cu	Cr 199 (43.78) N 230 (0.74) I	I 217 (−0.29) N[b]
6-Pd	Cr 257 (56.55) N 277 (0.41) I	I 270 (−0.11) N 226 (−43…38) Cr
6-Ni	Cr 225 (48.26) I	I[b]
6-VO	Cr 217 (62.62) N 242 (0.36)→I	I 240 (−0.25) N 176 (−29…58) Cr
5[a]	Cr_1 143 (31.09) I	I [136][c] (−0.41) N [112][d] SmC 96 (−20.84) Cr
7-Cu	Cr_1 134 (46.03) I	I [131] (−0.53) N[b]
7-Pd	Cr_1 172 (2.28) Cr_2 207 (52.31) I	I [188] (−0.24) N [184](−2.42) SmC 173 (−6.75) Cr

[a]Previously described thermal data for ligands **4** and **5**[21] are complemented and defined here by DSC measurements. [b]Vitrification of the sample may cause the absence of a crystallisation peak in DSC. [c]Monotropic phase transitions are shown in square brackets. [d]Merged in the DSC thermogram with a wide crystallisation peak.

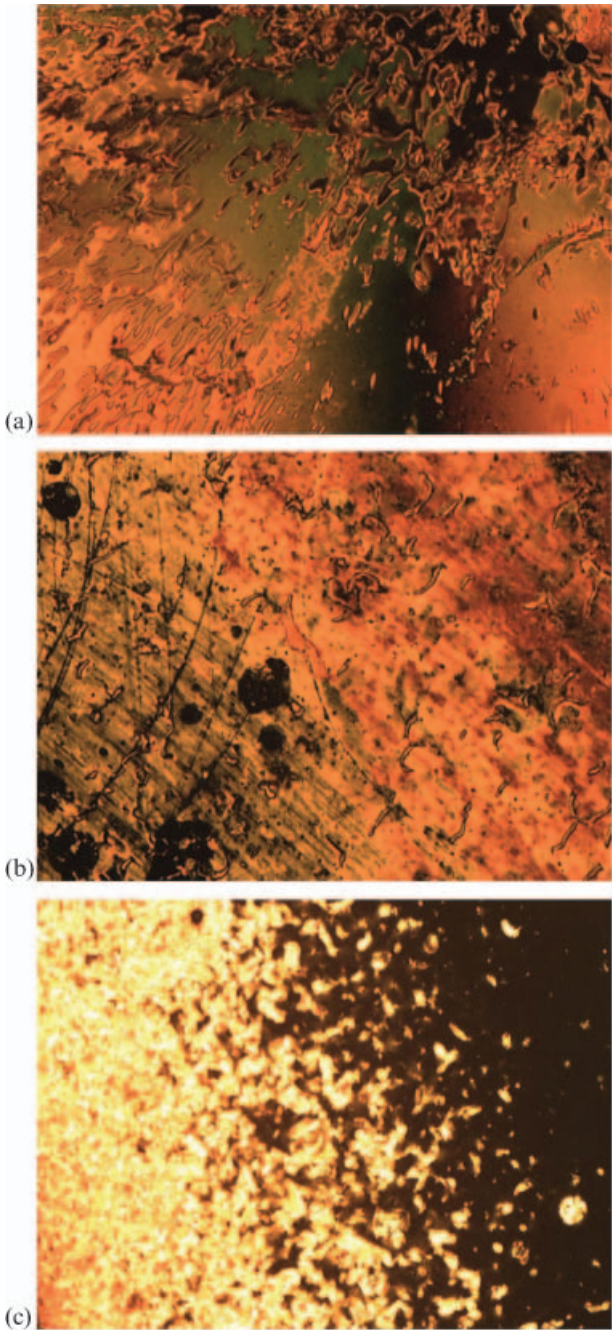

Figure 1. Microphotographs obtained upon cooling from the isotropic liquid state (× 10 magnification): (a) marbled texture of nematic in the *β*-aminovinylketone complex **7-Cu** at 120°C; (b) marbled-schlieren texture of nematic in the Schiff's base complex **6-VO**; (b) transition from nematic (homeotropically aligned dark area) to smectic C at 184°C in **7-Pd**.

mesophase. A comparison of complexes of the series **6** with the earlier reported isomorphic heteronuclear metal complexes containing unbridged ferrocene (*19*) clearly demonstrates the advantages of incorporating a propylidene group into the ferrocene fragment. Lower transition temperatures, more stable and broader mesophases are achieved in the heteropolynuclear metallomesogens synthesised in the present work. It is remarkable that the VO(IV) complex (*36–38*) showed an enantiotropic mesophase in a rather broad temperature range, in contrast to a monotropic nematic phase exhibited by the earlier reported isomorphic VO(IV) complex (*19*).

Another series of heteropolynuclear mesogenic systems of the present studies, which are based on the β-aminovinylketone chelates, showed only monotropic mesomorphism. Characteristic liquid crystal textures were observed under a polarising microscope (Figure 1), and the corresponding mesophase transitions were detected using a DSC instrument (Table 4). Complex **7-Cu** showed a monotropic nematic mesophase, and both nematic and smectic C mesophases were found in **7-Pd** upon cooling from the isotropic liquid state. In comparison with the earlier synthesised ferrocene-containing analogues (*20*) the present complexes with a ferrocenophane-containing *β*-aminovinylketone displayed lower phase transition temperatures.

4. Conclusions

Two [3]ferrocenophane derivatives containing promesogenic rod-like building units have been functionalised by salycilidene and *β*-aminovinylketone chelating sites, and then used as ligands for generating heteropolynuclear metallomesogenic systems. The synthesised complexes exhibited thermotropic nematic and smectic mesomorphism while they have favourable geometry for mesomorphism. Incorporating an aliphatic bridge into the terminal ferrocene fragment in the obtained mesogens substantially improves the thermal characteristics of the mesophases. The synthesised heteropolynuclear mesogenic materials are of special interest considering their potential in the area of new materials combining magnetic and liquid crystal properties.

Acknowledgements

This work has been supported by the program Brain Korea 21 (BK-21) and the Centre for Bioactive Molecular Hybrids (KOSEP). ONK is grateful to Professor Yuri Galyametdinov and Professor Willy Friedrichsen for initiating this work.

References

(1) Giroud-Godquin A.M.; Maitlis P.M. *Angew. Chem. Int. Ed. Engl.* **1991**, *30*, 375–402.
(2) Hudson S.A.; Maitlis P.M. *Chem. Rev.* **1993**, *93*, 861–885.
(3) Serrano J.L.(ed.) *Metallomesogens, Synthesis Properties and Applications*; Wiley-VCH: Weinheim, 1996.

(4) Bruce D.W. Metal-Containing Liquid Crystals. In *Inorganic Materials,* 2nd edition, Bruce D.W., O'Hare D. (Eds). Wiley: Chichester, 1996. pp. 429–515.
(5) Bruce D.W.; Donnio B.. *Metallomesogens*; Structure and Bonding 95; Springer: Berlin, 1999. pp. 193–247.
(6) Donnio B.; Guillon D.; Deschenaux R.; Bruce D.W. *Metallomesogens*; Comprehensive Coordination Chemistry II, 7, McCleverty J.A., Meyer T.J. (Eds). Elsevier: Oxford, 2003. pp. 357–627.
(7) Deschenaux R.; Monnet F.; Serrano E.; Turpin F.; Levelut A.-M. *Helv. Chim. Acta* **1998**, *81*, 2072–2077.
(8) Massiot P.; Impéror-Clerc M.; Veber M.; Deschenaux R. *Chem. Mater.* **2005**, *17*, 1946–1951.
(9) Imrie C.; Engelbrecht P.; Loubser C.; McCleland C.W. *Appl. Organomet. Chem.* **2001**, *15*, 1–15.
(10) Deschenaux R.; Goodby J.W. Ferrocene-Containing Thermotropic Liquid Crystals. In *Ferrocenes: Homogenous Catalysis, Organic Synthesis, Materials Science*; Togni A., Hayashi T. (Eds). Wiley-VCH: Weinheim, New York, 1995. pp. 471–495.
(11) Nakamura N.; Nio T.; Okabe T. *Mol. Cryst. Liq. Cryst.* **2006**, *460*, 85–92.
(12) Shen W.-C.; Wang Y.-J.; Cheng K.-L.; Lee G.-H.; Lai C.-K. *Tetrahedron* **2006**, *62*, 8035–8044.
(13) Apreutesei D.; Lisa G.; Scutaru D.; Hurduc N. *J. Optoelectr. Adv. Mater.* **2006**, *8*, 737–740.
(14) Campidelli S.; Perez L.; Rodriguez-Lopez J.; Barberá J.; Langa F.; Deschenaux R. *Tetrahedron* **2006**, *62*, 2115–2122.
(15) Brettar J.; Burgi T.; Donnio B.; Guillon D.; Klappert R.; Scharf T.; Deschenaux R. *Adv. Funct. Mater.* **2006**, *16*, 260–267.
(16) Apreutesei D.; Lisa G.; Akutsu H.; Hurduc N.; Nakatsuji S.; Scutaru D. *Appl. Organomet. Chem.* **2005**, *19*, 1022–1037.
(17) Senthil S.; Kannan P. *J. Polym. Sci., Part A: Polym. Chem.* **2002**, *40*, 2256–2263.
(18) Galyametdinov Yu.G.; Kadkin O.N.; Ovchinnikov I.V. *Rus. Chem. Bull.* **1990**, *39*, 2235.
(19) Galyametdinov Yu.; Kadkin O.; Prosvirin A. *Rus. Chem. Bull.* **1994**, *43*, 887–891.
(20) Kadkin O.N.; Galyametdinov Yu.G.; Rakhmatullin A.I.; Mavrin V.Yu. *Rus. Chem. Bull.* **1999**, *48*, 379–381.
(21) Kadkin O.; Galyametdinov Y.; Rakhmatullin A. *Mol. Cryst. Liq. Cryst.* **1999**, *332*, 109–118.
(22) Kahn O. *Angew. Chem. Int. Ed. Engl.* **1985**, *24*, 834–850.
(23) Buivydas M. *Phys. Status Solidi B* **1991**, *168*, 577–581.
(24) Kats E.I.; Lebedev V.V. *Mol. Cryst. Liq. Cryst.* **1999**, *209*, 329–337.
(25) Galyametdinov Y.; Ivanova G.; Griesar K.; Prosvirin A.; Ovchinnikov I.; Haase W. *Adv. Mater.* **1992**, *4*, 739–741.
(26) Liebsch S.; Oakley M.A.; Paschke R.; Sinn E. *Inorg. Chem. Commun.* **2002**, *5*, 525–526.
(27) Lelièvre D.; Bosio L.; Simon J.; André J.J.; Bensebaa F. *J. Am. Chem. Soc.* **1992**, *114*, 4475–4479.
(28) Pyzuk W.; Krowczynski A.; Chens L.; Gorecka E.; Bickczantaev I. *Liq. Cryst.* **1995**, *19*, 675–677.
(29) Krowczynski A.; Pociecha D.; Szydłowska J.; Przedmojski J.; Gorecka E. *Chem. Commun.* **1996**, 2731–2732.
(30) Serrette A.G.; Lai C.K.; Swager T.M. *Chem. Mater.* **1994**, *6*, 2252–2268.
(31) Szydłowska J.; Krowczynski A.; Gorecka E.; Pociecha D. *Inorg. Chem.* **2000**, *39*, 4879–4885.
(32) Binnemans K.; Lodewyckx K.; Donnio B.; Guillon D. *Chem. Eur. J.* **2002**, *8*, 1101–1105.
(33) Binnemans K.; Lodewyckx K. *Supramol. Chem.* **2003**, *15*, 485–494.
(34) Marcos M.; Omenat A.; Barberá J.; Duran F.; Serrano J.L. *J. Mater. Chem.* **2004**, *14*, 3321–3327.
(35) Binnemans K.; Lodewyckx K.; Donnio B.; Guillon D. *Eur. J. Inorg. Chem.* **2005**, 1506–1513.
(36) Werner A.; Friedrichsen W. *J. Chem. Soc. Chem. Commun.* **1994**, 365–366.
(37) Kadkin O.; Han H.; Galyametdinov Yu. *J. Organomet. Chem.* **2007**, *692*, 5571–5582.
(38) Kadkin O.; An J.; Han H.; Galyametdinov Y. *Eur. J. Inorg. Chem.* **2008**, 1682–1688.
(39) Schlögl K.; Mohar A.; Peterlik M. *Monatsh. Chem.* **1961**, *92*, 921–926.
(40) Rinehart Jr K.L.; Curby R.J.; Gustafson D.H.; Harrison K.G.; Bozak R.E.; Bublitz D.E. *J. Am. Chem. Soc.* **1962**, *84*, 3263–3269.
(41) Turbitt T.D.; Watts W.E. *J. Organomet. Chem.* **1972**, *46*, 109–117.
(42) Kadkin O.; Näther C.; Friedrichsen W. *J. Organomet. Chem.* **2002**, *649*, 161–172.